Springer

KSME

Journal of Mechanical Science and Technology 29 (5) (2015) 1869~1874
www.springerlink.com/content/1738-494x
DOI 10.1007/s12206-015-0407-4

A finite element analysis of turbulent eccentric stenotic flows by large eddy simulation †

Byoung Jin Jeon[1], Jungwoo Kim[2,*] and Hyoung Gwon Choi[3]

[1]*Department of Energy System, Seoul National University of Science and Technology, Seoul, 139-743, Korea*
[2]*Department of Mechanical System Design Engineering, Seoul National University of Science and Technology, Seoul, 139-743, Korea*
[3]*Department of Mechanical/Automotive Engineering, Seoul National University of Science and Technology, Seoul, 139-743, Korea*

(Manuscript Received December 31, 2014; Revised February 9, 2015; Accepted April 9, 2015)

Abstract

Blood flows with stenosis may cause turbulence. In such a case, vessels may be damaged by the turbulent flow because the velocity gradient of turbulent flow is large near the wall. It is very important to predict turbulence accurately. Generally, the shape of the stenotic vessel is quite complicated. Finite element method (FEM) is adopted because it is able to easily handle the stenotic vessel with unstructured meshes. Also, based on FEM, large eddy simulation (LES) is implemented to accurately solve turbulent flows in a vessel. To verify the accuracy of the LES technique developed, it is applied to the turbulent flow in an eccentric stenosis flow considered by Varghese et al. [1]. The simulation results showed that laminar flow occurs at the inlet region, whereas turbulence flow occurs after stenosis region. The present results show a reasonably good agreement with the DNS results of Varghese et al. [1].

Keywords: Large eddy simulation; Eccentric stenosis flow; Blood flow; Finite element method

1. Introduction

Blood in a vessel provides oxygen and nutrients to various organs of human body. Plaque growing in a vessel can make the area of flow passage small and then cause turbulence in blood flow. As a result, the abnormal blood flow due to plaque in a vessel may cause various kinds of diseases. A clear knowledge of fluid dynamics in stenotic vessels can help us understand the mechanism of disease progression and design better diagnostic procedures (Pal et al. [2]). In that respect, stenotic flows have been studied both numerically and experimentally by many researchers (Berger and Jou [3]).

Ahmed and Giddens [4] investigated stenotic flows experimentally for three area reduction rates (25%, 50%, 75%) of axisymmetric pipe at Re = 500, 1500 and 2000. Velocity and wall shear stress distributions at some selected positions were examined. Recently, Varghese et al. [1] simulated the experiment of Ahmed and Giddens [4] by using spectral element method at the area reduction rate of 75% at Re = 500, 1000. A grid independent solution at Re = 500 was found to be consistent with the experimental result of Ahmed and Giddens by using spectral element method with grid resolutions corresponding to 1.15~3 million points. On the other hand, Varghese et al. also studied the turbulent stenotic flow with an eccentric case at Re = 1000 in that this kind of the flow is relevant in the physiologic sense because actual arterial stenoses are likely to be asymmetric. Recently, the effect of eccentricity of stenotic flow was examined by Griffith et al. [5] at Re = 1-400. They reported that the flow field becomes more asymmetric as the eccentricity and Reynolds number increases and the magnitude of reverse flow increases as the eccentricity increases.

Some researchers have tried to employ turbulence models to solve stenotic flows because DNS may require a huge computing resource. In that respect, LES has been regarded as a viable method. Tan et al. [6] used constant Smagorinsky and dynamic Smagorinsky LES (Large eddy simulation) model to simulate the stenotic flow examined by Varghese et al. [1]. Although the results with constant Smagorinsky model were better than the other models, there were substantial deviations from the velocity profiles of experiment at some positions, which could be attributed to the fact that the flow undergoes a transition from laminar to a turbulence state in the post-stenotic region, and the turbulent flows are only weakly turbulent (Fischer et al. [7]). In that respect, the Vreman model recently proposed by Vreman [8] has a good feature that the SGS eddy viscosity is automatically zero at the flow region where the SGS dissipation should be zero.

*Corresponding author. Tel.: +82 2 970 6856
E-mail address: kimjw@seoultech.ac.kr
† This paper was presented at the 10th ACFD, Jeju, Korea, October 2014.
Recommended by Guest Editor Hyoung-Gwon Choi

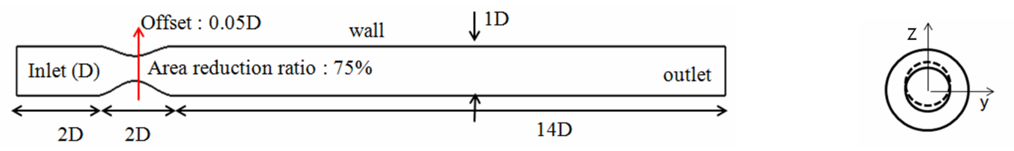

(a) x-z plane (b) y-z plane

Fig. 1. Schematic of the eccentric stenosis model [1].

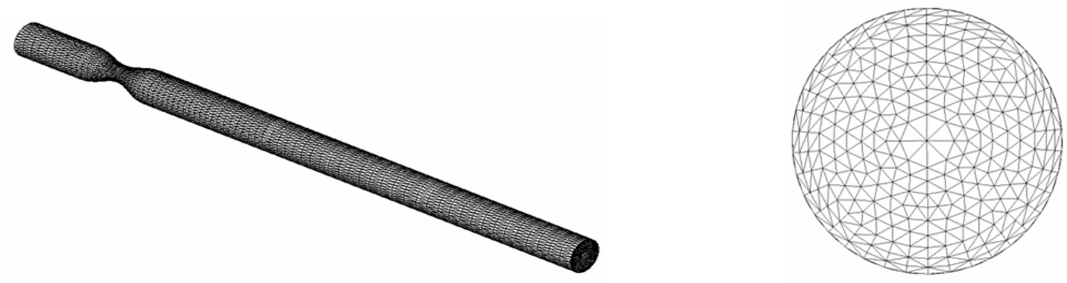

(a) 3-D mesh (b) y-z plane mesh at the inlet

Fig. 2. Mesh of the eccentric stenosis model.

Therefore, the objective of this study was to develop the LES technique with the Vreman model as SGS models to accurately predict the turbulent blood flow in vessels. For simulations, we considered finite element method allowing for geometric flexibility because the shape of the vessels could be quite complicated. Finally, the performance of the present LES technique was assessed against the previous studies.

2. Numerical method

In the present study, a 3-step finite element method (FEM) based on P2P1 element is employed to solve the eccentric stenotic flows. In the 3-step FEM, Galerkin and Crank-Nicolson methods are employed for spatial and temporal discretizations, respectively. Therefore, this method is third/second order accurate in space/time and unconditionally stable. More details of the present 3-step FEM are in Cho et al. [9]. Fig. 1 shows the schematic diagram for the computational domain and coordinate system. As shown in Fig. 1, in this study the eccentric stenotic flow in which stenosis axis was offset from the main vessel axis by 0.05D, which is the same as that by Varghese et al. [1]. As the boundary conditions, at the inlet the steady laminar parabolic velocity profile was imposed, and at the outlet the traction free condition was applied. Also, the wall of the stenotic vessel was regarded as rigid. As shown in Fig. 2, unstructured mesh based on tetrahedron was used. The numbers of node and cell are 308721 and 225498, respectively. Velocity variables were interpolated by quadratic basis function and pressure by linear.

In the present study, the Reynolds number based on the mean inlet velocity (u_i) and the main diameter of the stenotic vessel is 1000. At this Reynolds number, the flow in the post-stenotic region becomes turbulent. The typical Reynolds number range of blood flow varies from O(1) in small arterioles to O(10^3) in the largest artery, the aorta [10]. For blood flow, density and viscosity of the blood are considered as 1050 kg/m^3 and 0.004 kg/m-s, respectively [11]. As for LES model, the subgrid-scale model developed by Vreman [8] is considered. Thanks to the good feature of the Vreman model already mentioned, it has been successfully applied to some bio-fluid-dynamic problems (Choi et al. [12]). In the Vreman model [8], the eddy viscosity is defined as

$$\nu_T = C_v \sqrt{\Pi_\beta / \overline{\alpha_{ij}}\,\overline{\alpha_{ij}}}$$

$$(\overline{\alpha_{ij}} = \partial \overline{u_j} / \partial x_i,\ \Pi_\beta = \beta_{11}\beta_{22} - \beta_{12}^2 + \beta_{11}\beta_{33} - \beta_{13}^2 + \beta_{22}\beta_{33} - \beta_{23}^2,$$

$$\beta_{ij} = \sum_{m=1}^{3} \Delta_m^2 \overline{\alpha_{mi}}\,\overline{\alpha_{mj}}\ ).$$

Here, C_v is the Vreman model [8] coefficient, and in this study it is set to be 0.07.

Since long-term simulations are necessary for averaging process of the present LES, parallel computations based on domain decomposition and MPI method have been conducted. We extended the parallel algorithm developed by Choi et al. [13] for P1P1 splitting formulation to the present method for P2P1 splitting technique.

3. Results and discussion

Fig. 3 shows the instantaneous vorticity magnitude ($|\overline{\omega}| = \sqrt{\omega_i \omega_i}$) contours of the flow in the eccentric stenosis model. For comparison, the previous results are included from the DNS performed by Varghese et al. [1] and the LES by Varghese et al. [14] with the SGS model implemented in Fluent 6.2. As shown in Fig. 3, the shear layer surrounded by a long, thin recirculation zone is developed at the stenosis throat, which was already observed in previous studies (Sherwin and Blackburn [15] ; Varghese et al. [1] ; Vetel et al. [16]). The

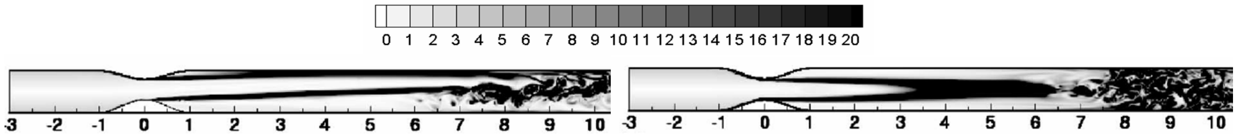

(a) Varghese et al. [1] (x-z plane, y = 0; DNS) (b) Varghese et al. [1] (x-y plane, z = 0; DNS)

(c) Varghese et al. [14] (x-z plane, y = 0; Fluent LES) (d) Varghese et al. [14] (x-y plane, z = 0; Fluent LES)

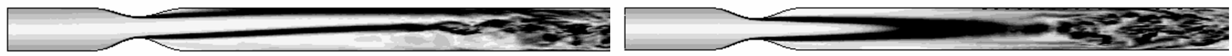

(e) Present (x-z plane, y = 0) (f) Present (x-y plane, z = 0)

Fig. 3. Comparison of instantaneous vorticity magnitude contours of the eccentric stenosis model.

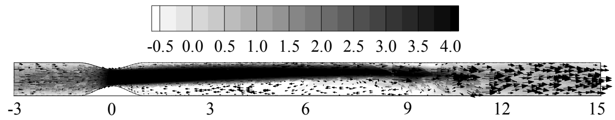

Fig. 4. Time-averaged axial velocity contours and vector field of the eccentric stenosis.

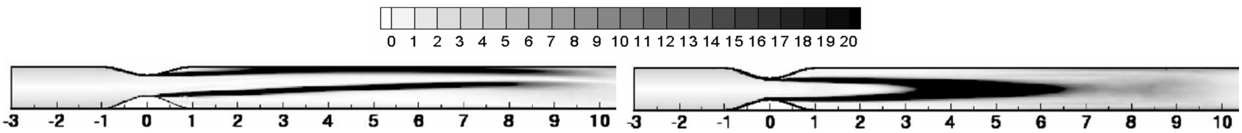

(a) Varghese et al. [1] (x-z plane, y = 0; DNS) (b) Varghese et al. [1] (x-y plane, z = 0; DNS)

(c) Varghese et al. [14] (x-z plane, y = 0; Fluent LES) (d) Varghese et al. [14] (x-y plane, z = 0; Fluent LES)

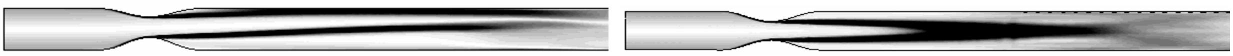

(e) Present (x-z plane, y = 0) (f) Present (x-y plane, z = 0)

Fig. 5. Comparison of time-averaged vorticity magnitude contours of the eccentric stenosis model.

recirculation zone can be identified more clearly in Fig. 4. Contrary to the previous studies for an axisymetric stenosis model (Varghese et al. [1]), the recirculation zone only exists in the lower side corresponding to the opposite side of the eccentricity. Also, under the influence of the eccentricity, the shear layer is deflected toward the upper side. The inclination angle of the shear layer is around 4^o, which is similar to that seen in the previous result. The shear layer almost remains until x = 8-9, and then the transition to turbulence is observed in downstream. Although small-scale structures in downstream (x = 10-13) could not be well resolved in this study as compared to the previous one, the overall feature of the vortical structures observed in the present paper is also seen in Refs. [1, 14].

Fig. 5 shows the time-averaged vorticity magnitude contours through the eccentric stenosis model. In the current simulation, the time-averaging is taken during the non-dimensional time interval of Tu_i/D = 140. As observed by Varghese et al. [1, 14], the localized transition occurs after approximately x = 4. Correspondingly, the ratio of the turbulent viscosity and the fluid viscosity increases nearly at that location as shown in Fig. 6. Based on the ratio of the turbulent eddy viscosity and laminar viscosity (v_t/v), the transition starts inside the shear layer. As the flow goes downstream, the whole flow becomes turbulent.

For further validation of the present simulation, the turbulence statistics are presented. Figs. 7 and 8 show the mean streamwise velocity and streamwise velocity fluctuations, respectively. They are compared against those given by Varghese et al. [1, 14] (DNS and k-w RANS model) and Tan et al. [6] (Smagorinsky and dynamic Smagorinsky models). Here, x-z plane is the symmetric plane of the stenosis model given. As shown in Figs. 7 and 8, the present results are in a reasonably good agreement with the previous DNS results, which show that the Vreman model is successfully implemented in FEM framework considered in the present study. The velocity distributions in x-z plane clearly show the effect of eccentricity, but those in x-y plane do not because the stenosis model is only asymmetric in x-z plane. As said above, negative velocity

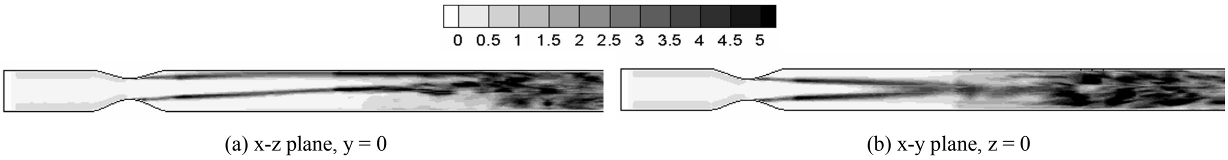

Fig. 6. Instantaneous v_t/v contours of the eccentric stenosis model (The instantaneous time is the same as that in Fig. 1).

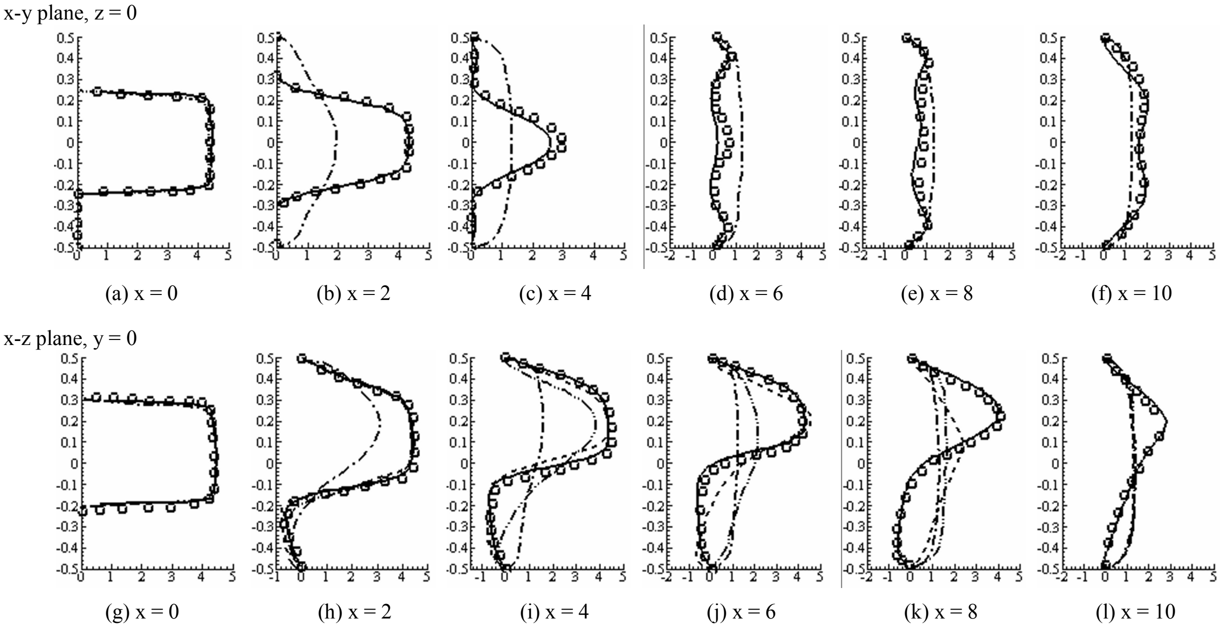

Fig. 7. Time-averaged axial velocity profiles, u/u_i along the several axial locations (Solid line : Vreman model, circle : DNS [1], dash-dot : k-w model [14], dash : Smagorinsky model [6], dash-dot-dot : Dynamic Smagorinsky model [6]).

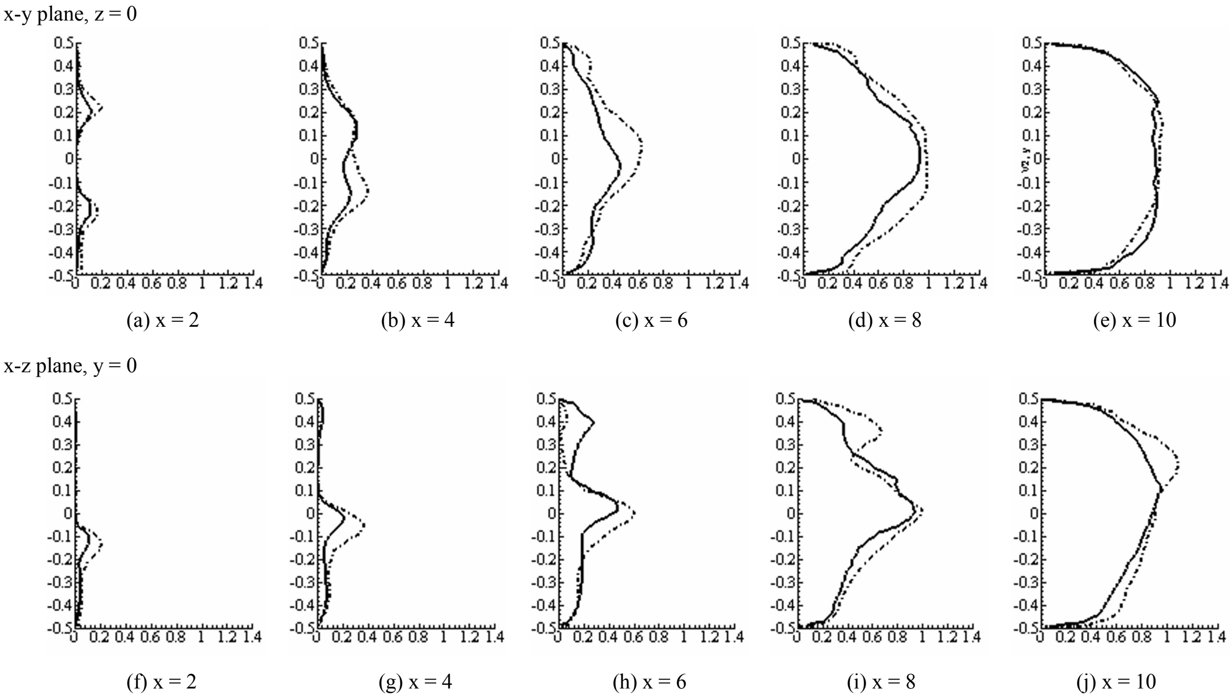

Fig. 8. Root-mean-square axial velocity profiles (Solid line : Vreman model, dash-dot : DNS[1]).

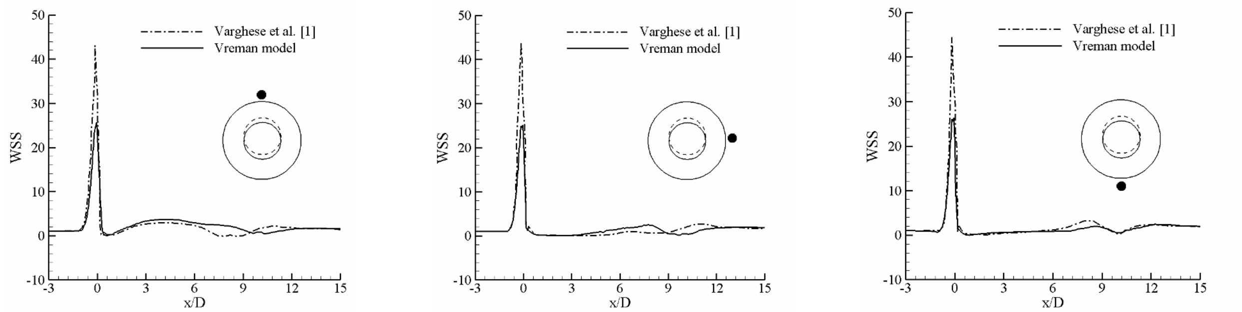

(a) (b) (c)

Fig. 9. Time-averaged axial wall shear stress magnitude along the vessel walls, normailized by the value upstream of the stenosis at three different azimuthal locations.

related to the existence of the recirculation zone is observed in the lower side in the region of x = 6, 8. At x = 10, the recirculation zone disappears so the negative velocity does not exist. Also, the difference between the time-averaged velocities in x-z and x-y planes become smaller in farther downstream section as the jet disappears and the transition to the turbulence occurs.

In the problem related to the stenosis model, another relevant physical property is the skin friction at the wall. The turbulent motion in a vessel affects the constituent of the blood as well as the function of the endothelial cell layer, at which the wall shear stress is recognized as a mediator of the local hemodynamics to the inner layer Gardhagen et al. [17].

Fig. 9 shows the distribution of the axial component of the time-averaged wall skin friction along the vessel walls at three different azimuthal locations. The value is normalized by that upstream of the stenosis. For comparison, the previous results by Varghese et al. [1] are included. Overall, the wall shear stresses in the present study show reasonably good agreement with those obtained in the previous DNS study (Varghese et al. [1]) although the peak value in the present study is a little smaller than that in the previous one. As shown in this figure, just in front of the throat, the wall skin friction has the maximum value by a factor of around 30 as compared to that at the inlet. However, right after the throat, the wall skin friction rapidly decreases and then as the flow moves within the diverging section the wall shear stress returns to that at the inlet. Also, the wall shear stress is affected by the eccentric of the stenosis model. At 0 < x < 8, under the influence of the deflecting jet, the wall shear stress on the side of the eccentricity is larger than those on the other locations. However, after x = 8, the influence of the eccentricity disappears, and the wall shear stress is nearly independent on the azimuthal locations.

4. Conclusions

To perform large eddy simulations of the turbulent flow in a stenosis model, a subgrid-scale model based on the Vreman model [8] was implemented into a finite element method. To validate the performance of the present large eddy simulation technique, the turbulent flow in the stenosis model considered by Varghese et al. [1] was simulated. The simulation results show that laminar flow occurs at the inlet region, whereas turbulent flow occurs after the stenosis region. Compared to the previous results, the present results show a reasonably good agreement in terms of the vortical structures as well as the turbulence statistics such as the time-averaged streamwise velocity and axial wall shear stress.

Acknowledgment

This work was supported by the ICT R&D program of MSIP/IITP. [10044910, Development of Multi-modality Imaging and 3D Simulation-Based Integrative Diagnosis-Treatment Support Software System for Cardiovascular Diseases].

Nomenclature

Re	: Reynolds number
D	: Main diameter of the stenotic vessel
T	: Sampling time for averaging
u	: Axial velocity
u_i	: Mean inlet velocity
C_v	: Vreman model coefficient
ν	: Kinematic viscosity of fluid
ν_t	: Turbulent eddy viscosity
ω	: Vorticity

References

[1] S. S. Varghese, S. H. Frankel and P. F. Fischer, Direct numerical simulation of stenotic flow: Part 1. Steady flow, *J. Fluid Mech.*, 582 (2007) 253-280.

[2] A. Pal, K. Anupindi, Y. Delorme, N. Ghaisas, D. A. Shetty and S. H. Frankel, Large eddy simulation of transitional flow in an idealized stenotic blood vessel: evaluation of subgrid scale models, *J. Biomech. Eng.*, 136 (2014) 071009.

[3] S. A. Berger and L.-D. Jou, Flows in stenotic flows, *Annu. Rev. Fluid Mech.*, 32 (2000) 347-382.

[4] S. A. Ahmed and D. P. Giddens, Velocity measurements in

steady flow through axisymmetric stenoses at moderate Reynolds numbers, *J. Fluid Mech.,* 16 (1983) 505-516.
[5] M. D. Griffith, T. Leweke, M. C. Thompson and K. Hourigan, Effect of small asymmetries on axisymmetric stenotic flow, *J. Fluid Mech.*, 721 (2013).
[6] F. P. P. Tan, N. B. Wood, G. Tabor and X. Y. Xu, Comparison of LES of steady transitional flow in an idealized stenosed axisymmetric artery model with a RANS transitional model, *J. Biomech. Engrg.*, 133 (2011).
[7] P. F. Fischer, F. Loth, S. E. Lee, S.-W. Lee, D. S. Smith and H. S. Bassiouny, Simulation of high-Reynolds number vascular flows, *Comput. Methods Appl. Mech. Engrg.*, 196 (2007) 3049-3060.
[8] A. W. Vreman, An eddy-viscosity subgrid-scale model for turbulent shear flow: algebraic theory and application, *Phys. Fluids*, 16 (2004) 3670-3681.
[9] M. H. Cho, H. G. Choi, J. Y. Yoo and J. I. Park, Study on the segregation algorithms of the incompressible Navier-Stokes equations using P1P2/P2P1 finite element formulation, *Trans. of the KSME (B)*, 30 (2006) 262-269.
[10] D. N. Ku, Blood flow in arteries, *Annu. Rev. Fluid Mech.*, 29 (1997) 399-434.
[11] K. M. Guleren, Numerical flow analysis of coronary arteries through concentric and eccentric stenosed geometries, *J. Biomech*, 46 (2013) 1043-1052.
[12] J. Choi, M. H. Tawhai, E. A. Hoffman and C.-L. Lin, On intra- and intersubject variabilities of airflow in the human lungs, *Phys. Fluids*, 21 (2009) 101901.
[13] H. Choi, S. Kang and J. Y. Yoo, Parallel large eddy simulation of turbulent flow around MIRA model using linear equal-order finite element *method, Int. J. Numer. Meth. Fluids*, 56 (2008) 823-843.
[14] S. S. Varghese, S. H. Frankel and P. F. Fischer, Modeling transition to turbulence in eccentric stenotic flow, *J. Biomech. Engrg.*, 130 (2008) 014503.
[15] S. J. Sherwin and H. M. Blackbum, Three-dimensional instabilities of Steady and pulsatile axisymmetric in a closed stenotic flows, *J. Fluid Mech.*, 533 (2005) 297-327.
[16] J. Vetel, A. Garon, D. Pelletier and M. I. Farinas, Asymmetry and transition to turbulence in a smooth axisymmetric constriction, *J. Fluid Mech.*, 607 (2008) 351-386.
[17] R. Gardhagen, J. Lantz, F. Carlsson and M. Karlsson, Quantifying turbulent wall shear stress in a stenosed pipe using large eddy simulation, *J. Biomech. Engrg.*, 132 (2010) 061002.

Byoung-jin Jeon received a Ph.D. at Seoul National University of Science and Technology majoring in computational fluid dynamics based on finite element method. He is currently a Post-Doc in the integrative cardiovascular imaging research center of Yonsei University.

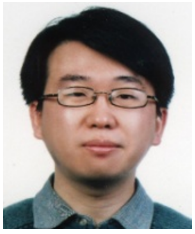

Jungwoo Kim obtained his B.S., M.S. and Ph.D. degrees at the Department of Mechanical Engineering, Seoul National University, Korea, in 1999, 2001 and 2005. Dr. Kim is currently an assistant professor at the Department of Mechanical System Design Engineering, Seoul National University of Science and Technology.

Hyoung-gwon Choi received a Ph.D. at Seoul National University majoring in computational fluid dynamics based on finite element method. He is currently a professor in the department of mechanical engineering of Seoul National University of Science and Technology.